Bioorganic & Medicinal Chemistry 19 (2011) 7365–7373

Contents lists available at SciVerse ScienceDirect

Bioorganic & Medicinal Chemistry

journal homepage: www.elsevier.com/locate/bmc

Synthesis and bio-evaluation of human macrophage migration inhibitory factor inhibitor to develop anti-inflammatory agent

Athar Alam [a,†], Chinmay Pal [a,†], Manish Goyal [a], Milan Kumar Kundu [b], Rahul Kumar [a], Mohd Shameel Iqbal [a], Sumanta Dey [a], Samik Bindu [a], Souvik Sarkar [a], Uttam Pal [c], Nakul C. Maiti [c], Susanta Adhikari [d,*], Uday Bandyopadhyay [a,*]

[a] Department of Infectious Diseases and Immunology, Indian Institute of Chemical Biology, 4 Raja S. C. Mullick Road, Jadavpur, Kolkata 700 032, West Bengal, India
[b] Department of Chemistry, University of Burdwan, Golapbag, Burdwan 713 104, West Bengal, India
[c] Department of Structural Biology & Bio-Informatics Division, Indian Institute of Chemical Biology, 4 Raja S. C. Mullick Road, Jadavpur, Kolkata 700 032, West Bengal, India
[d] Department of Chemistry, University of Calcutta, 92, A. P. C. Road, Kolkata 700 009, West Bengal, India

ARTICLE INFO

Article history:
Received 30 August 2011
Revised 17 October 2011
Accepted 18 October 2011
Available online 24 October 2011

Keywords:
Human macrophage migration inhibitory factor (huMIF) inhibitor
Tautomerase activity
Nuclear factor kappa-B (NF-κB)
Nitric oxide synthase
Nitric oxide
Inflammation

ABSTRACT

Macrophage migration inhibitory factor (MIF), a pro-inflammatory cytokine, is involved in the development of an array of inflammatory disorders including rheumatoid arthritis, inflammatory bowel disease, psoriasis, multiple sclerosis and sepsis. The synthesis of MIF-inhibitor is a rationale approach to develop novel anti-inflammatory agent to treat multitude of inflammatory diseases. In this work, we have synthesized and evaluated MIF-inhibitory activity of a series of small molecules containing isoxazoline skeleton. Mode of binding of this inhibitor to human MIF (huMIF) was determined by docking studies. The synthesized molecules inhibit tautomerase activity of huMIF. The anti-inflammatory activity of the most active inhibitor, 4-((3-(4-hydroxy-3-methoxyphenyl)-4, 5-dihydroisoxazol-5-yl) methoxy) benzaldehyde (**4b**) was evaluated against huMIF-induced inflammation in a cellular model (RAW 264.7 cell). Compound **4b** significantly inhibits huMIF-mediated NF-κB translocation to the nucleus, up-regulation of inducible nitric oxide synthase and nitric oxide production in RAW 264.7 cell which are the markers for inflammation. The compound **4b** is not cytotoxic as evident from cell viability assay. Hence, the compound **4b** has potential to be a novel anti-inflammatory agent.

1. Introduction

Pleiotropic pro-inflammatory cytokine macrophage migration inhibitory factor (MIF) is a validated target against pathogenesis of many pro-inflammatory and autoimmune disorders.[1,2] MIF was originally identified as a T-cell-derived factor responsible for the inhibition of macrophage migration in experiments designed to characterize delayed-type hypersensitivity.[3,4] MIF is found to be expressed by a variety of cells including eosinophils, epithelial cells, endothelial cells, lymphocytes and macrophage.[5–9] Stimulation of MIF in vivo with endotoxin promotes secretion from pools of stored protein within the cell causing immediate amplification of the pro-inflammatory response.[10] The pro-inflammatory activities of MIF include induction of TNF-α, IL-1, IL-8, and NO release from macrophages and the induction of cyclooxygenase with the subsequent production of prostaglandin E2 (PGE2).[1,11] As a consequence of its induction of pro-inflammatory molecules, MIF has the potential to be involved in the pathogenesis of a range of immune-mediated inflammatory diseases including rheumatoid arthritis, atherosclerosis, diabetes, sepsis, cancer, colitis, inflammatory bowel disease, multiple sclerosis, asthma, inflammatory liver disease, systemic lupus erythematosus and several infectious diseases.[12–14] Tautomerase activity of MIF as well as the interaction of MIF with the CD-74 receptor is reported for the cause of inflammatory disorder.[15–19] Thus, MIF could be the one of the best therapeutic target to treat diseases originated from MIF-mediated inflammation. Therefore, molecule which will inhibit MIF activity will be of great value to combat above-mentioned MIF-mediated inflammation. After consideration of a series of heterocycles as a core structure, the 3,5-disubstituted isoxazoline was selected for further studies, because it is evident from literature that the molecules having isoxazoline skeleton are in general the potent MIF-inhibitor.[20–26] Here, we report the synthesis and evaluation of such small molecules having isoxazoline skeleton that inhibit the tautomerase activity of human MIF (huMIF). The compound **4b** appeared to be the most active huMIF tautomerase inhibitor and it also inhibits the huMIF-induced NF-κB translocation to the nucleus, up-regulation of inducible nitric oxide synthase (iNOS) and

* Corresponding authors. Tel.: +91 33 23509937; fax: +91 33 23519755 (S.A.); tel.: +91 33 24733491; fax: +91 33 24730284 (U.B.).
E-mail addresses: adhikarisusanta@yahoo.com (S. Adhikari), ubandyo_1964@yahoo.com (U. Bandyopadhyay).
† These authors contributed equally.

0968-0896/$ - see front matter © 2011 Elsevier Ltd. All rights reserved.
doi:10.1016/j.bmc.2011.10.056

nitric oxide (NO) production in RAW 264.7 cells. Finally, our data suggest that this compound **4b** could be a potential anti-inflammatory molecule because the huMIF inhibition led to the inhibition of huMIF-mediated inflammatory diseases.

2. Results and discussion

2.1. Chemistry

A series of small molecules (**1a–c**, **2a**, **2b**, **3a–f**, **4a–b** and **5a**) having isoxazoline skeleton have been synthesized using 1,3-dipolar cycloaddition chemistry. The key intermediate 4-methoxybenzaldehyde oxime, 4-hydroxy-3-methoxybenzaldehyde oxime and 3,4-dimethoxybenzaldehyde oxime required for the synthesis of different dihydro-isoxazoles (**1a–c**) were synthesized from separate reactions between 4-hydroxy benzaldehyde, *p*-anisaldehyde, vanilin and 3,4-dimethoxybenzaldehyde, respectively with hydroxylamine hydrochloride in presence of sodium acetate in good yields. Then, **1a–c** were synthesized by condensation of vinyl acetic acid with respective aforementioned oximes in presence of N-chlorosuccinimide and triethyl amine in DMF (Scheme 1).[20] In a similar manner, **2a** and **2b** were synthesized subsequently by condensation of 3,4-dimethoxybenzaldehyde oxime with methyl acrylate and but-3-en-2-one, respectively (Scheme 2). With the objective of synthesizing various isoxazoles with aliphatic and aromatic substitutions, intermediate **1b** was reacted further with different amines such as 5-methoxy tryptamine, 4-amino-2-isopropyl-5-methylphenol and alcohols such as 2-isopropyl-5-methylphenol and *N*-(4-hydroxyphenyl)acetamide, respectively using standard EDC coupling protocol (EDC-HCl, HOBt, Et_3N) to yield the desired products **(3a–d)** as depicted in Scheme 3. In a separate study, the esterification of intermediate **1b** was accomplished with TMSCl using alcohols such as methanol and butanol, respectively to give the desired products **3e**, **3f** (Scheme 3). In order to synthesize **4a** and **4b**, the intermediate 4-hydroxy-3-methoxybenzaldehyde oxime was reacted in parallel with 2-(allyloxy)-1-isopropyl-4-methylbenzene and 4-(allyloxy)benzaldehyde (prepared by the separate allylation of 2-isopropyl-5-methylphenol and 4-hydroxy benzaldehyde in presence of allyl bromide and potassium carbonate in acetone), respectively in presence of N-chlorosuccinimide and triethyl amine in DMF (Scheme 4). To the end, bis-isoxazole derivative, **5a** was synthesized by the condensation of **4c**[20] (prepared from **1a** using TMSCl and methanol) with **1b** using standard EDC coupling method (Scheme 5). The structure of various synthesized compounds was assigned on the basis of different spectral data (Supplementary data).

2.2. Biological evaluation

2.2.1. Inhibition of human macrophage migration inhibitory factor (huMIF) by the synthesized small molecule

Tautomerase activity of huMIF is responsible for many pro-inflammatory diseases.[18,21,23,26] Therefore, the molecules that can inhibit the tautomerase activity of huMIF can be a good choice against huMIF-induced inflammatory diseases. The data indicated that the series of synthesized small molecules (**1a–c**, **2a**, **2b**, **3a–f**, **4a–b** and **5a**) inhibited tautomerase activity of huMIF. Among these compounds **1c** (IC_{50} 10.2 ± 1.5 μM), **3f** (IC_{50} 11.2 ± 1.7 μM) and **4b** (IC_{50} 7.3 ± 0.98 μM) were found to be active compared to the other compounds (Table 1). From comparative analysis of IC_{50} it is clear that among these synthesized compounds; **4b** is appeared to be the most active huMIF inhibitor. Since **4b** appears to be the most active among all the synthesized compounds, it is assumed that the presence of formyl group along with isoxazoline skeleton in small molecule might play an important role for its huMIF inhibitory activity. Furthermore, data indicate that ester analogues are more potent than the amide counterpart (Table 1). Moreover, among ester analogues **(2a**, **3c–f**, **5a**), aliphatic esters preferably with long chain seems to be better inhibitor. However, acid derivatives (**1a–c**) bearing hydroxy as well as methoxy functionality in the aromatic substitution appear to be more potent in comparison to hydroxy or methoxy alone.

Although compound **1c** and **3f** exhibit more or less same activity in vitro, our aim was to design not only tautomerase inhibitor but an inhibitor which will be more effective in cellular or in vivo system with enhanced bioavailability. That is why compound **4b** was synthesized by substituting formyl group along with the isoxazoline skeleton and only compound **4b** was subjected for further detailed biological evaluation for huMIF-induced inflammation and mechanistic studies.

2.2.2. Prediction of binding site and affinity of 4b with huMIF through molecular modeling

To identify the binding site of **4b** with huMIF, molecular docking study was performed. huMIF, a homo-trimer with radial symmetry (Fig. 1A), contains three active sites. These active sites are narrow, deep and lie in the junction of two monomeric units and towards the N and C terminal end of the protein. Figure 1A was generated using PyMOL and PDB entry 1GD0 (resolution 1.5 Å) for the dock study.

Compound **4b** has two stereo-isomers (*R* and *S*). Docking simulations were carried out with both the isomers and both of them were found to bind to the active site of the enzyme. The docked conformation shown in Figure 1A is *R*-**4b**. The magnified view of the interacting site of the molecule *R*-**4b** is shown in Figure 1B. To get maximum reliable prediction, we used two well known docking programs, AutoDock 4 and PatchDock. PatchDock reproduced the results as obtained with AutoDock 4 with RMSD 2.897 Å for *R*-**4b** and 2.643 Å for *S*-**4b**, respectively. Although the *R*-form is linear while *S* is bent, the best docked conformations of both the isomers were found to align the same end inside the groove (data not shown). AutoDock study indicates that three residues Lys32, Ile64 and Asn97 in the active site are involved in the binding with the compound **4b** through hydrogen bonding whereas the PatchDock indicates the involvement of Pro1 also. Proline 1 is already reported to be involved in the catalysis of

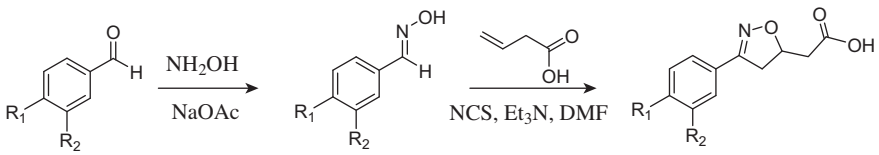

R_1 = OH, **R_2 =** H;(**1a**)
R_1 = OMe, **R_2**= H; (**1b**)
R_1 = OH, **R_2**= OMe; (**1c**)

Scheme 1. Chemical synthesis of **1a–c**.

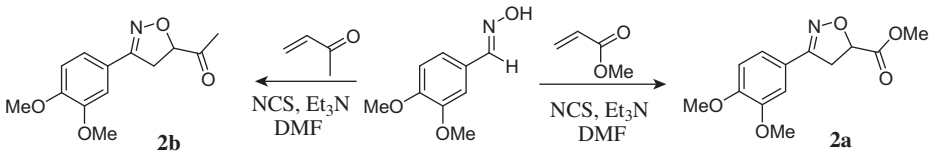

Scheme 2. Chemical synthesis of **2a**, **2b**.

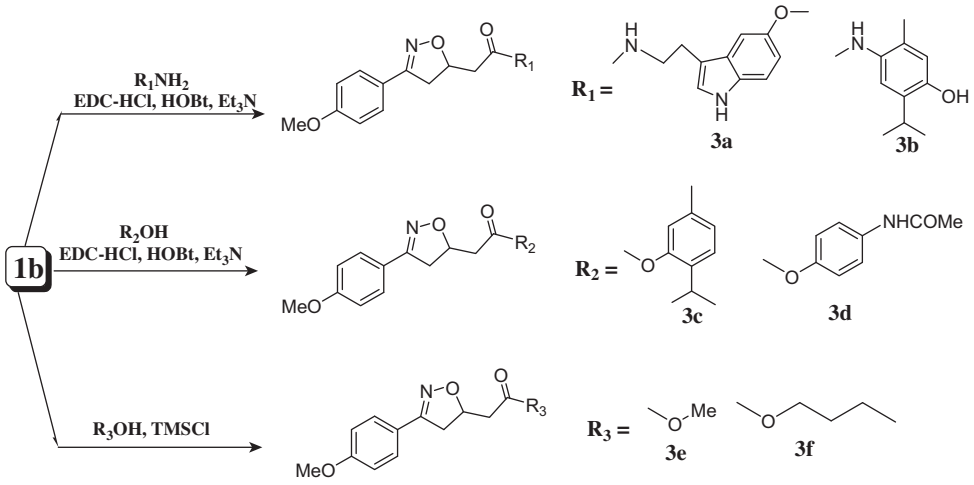

Scheme 3. Chemical synthesis of **3a–f**.

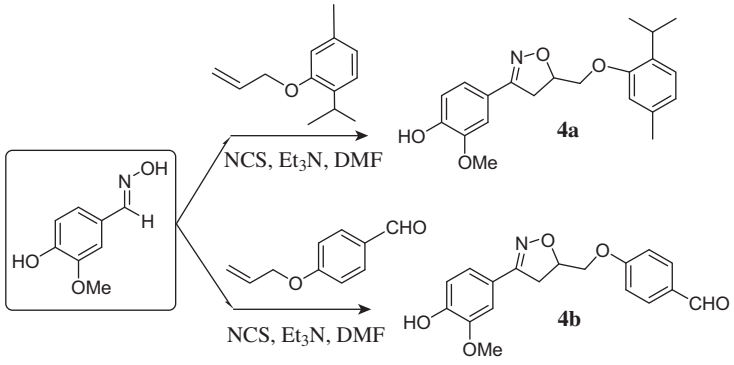

Scheme 4. Chemical synthesis of **4a**, **4b**.

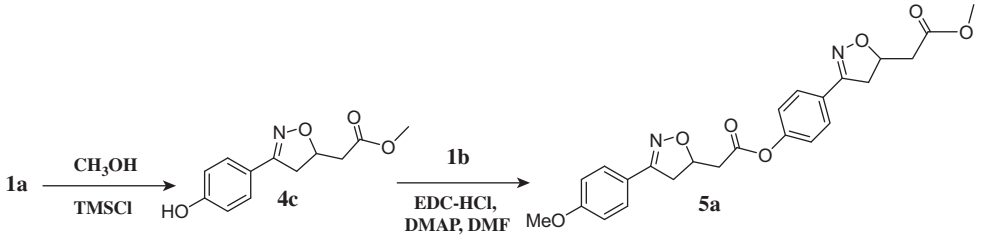

Scheme 5. Chemical synthesis of **5a**.

tautomerase activity of huMIF.[27] The binding free energies and the change in the accessible surface area (ASA) of the ligands are tabulated in the Table 2. K_i (inhibitor's dissociation constant) values are 5.44 μM and 1.57 μM for *R*- and *S*-**4b**, respectively, which indicate strong binding. It is also supported by the experimentally determined low IC_{50} value for **4b**.

Data indicate that the hydrophobic interactions, Van der Waals attraction and hydrogen bond formation are the major contributing factors in this binding. *R*-**4b** is found to interact with all the three binding site residues of huMIF. A strong hydrogen bond is formed between Chain-B:Lys32:Hζ2 of MIF with oxygen (O) of isoxazoline ring in both *R*- and *S*-**4b** (length, *l* = 1.949 Å; donor-hydrogen-

Table 1
Inhibition of tautomerase activity of huMIF by the synthesized molecule (**1a–5a**)

Compound	IC_{50} (μM) ($M \pm SEM$)
1a	15.2 ± 1.4
1b	16.7 ± 1.71
1c	10.2 ± 1.5
2a	25.2 ±1.82
2b	35.4 ± 2.47
3a	NA
3b	NA
3c	55.3 ± 3.24
3d	NA
3e	19.7 ± 2.11
3f	11.2 ± 1.7
4a	NA
4b	7.3 ± 0.98
5a	37.2 ± 2.5

Table 2
Binding parameters as predicted by AutoDock 4 and PatchDock

Ligand	Binding parameters	AutoDock 4	PatchDock
R-**4b**	$\Delta G°$ (kJ mol^{-1})	−30.04	−39.81
	ΔASA_{Ligand} (%)	73.12	71.47
S-**4b**	$\Delta G°$ (kJ mol^{-1})	−33.14	−47.05
	ΔASA_{Ligand} (%)	73.98	79.09

acceptor angle, $\theta = 154.614°$ with *R*-**4b** and $l = 1.921$ Å; $\theta = 151.734°$ with *S*-**4b**). The other two donor:acceptor pairs are Chain-A:Asn97:Hδ2 of huMIF with O of formyl group and Chain-B:Ile64:HN with O adjacent to isoxazoline ring (Fig. 1B). Despite of the structural variation imparted by the chiral C of isoxazoline ring, in both the *R* and *S* form bound to the active site the spatial arrangement of the three hydrogen bond acceptor O atoms are very similar. It accounts for their similar hydrogen bonding interactions. The positioning of these three O atoms on **4b**, therefore, is crucial for the strong binding with the three active site residues. The change in the ASA gives further insight into the mechanism of interactions. More change indicates more solvent exclusion and thus hydrophobic interaction. The model of the complex also suggests the type of enzyme inhibition. Compound **4b** occupies the same site as the substrate does, preventing substrate binding to the enzyme and as the K_i value is low, inhibition is strong. Finally, data indicate that the compound **4b** interacts with the four different amino acid residues (Lys32, Ile64, Asn97 and Pro1) at the active site which may be involved in the modulation of the huMIF activity including the tautomerase activity as indicated by the involvement of Pro1, a well documented residue at the active site for the tautomerase activity.[27]

2.2.3. Compound 4b inhibits huMIF-induced translocation of nuclear factor kappa-B (NF-κB) to nucleus

Nuclear factor kappa-B (NF-κB) is a ubiquitous transcriptional factor and promotes the transcription of about 150 genes.[28] Many of these genes are pro-inflammatory, including cytokines, adhesion molecules and nitric oxide synthase.[29] NF-κB translocation to nucleus by different cytokines including huMIF has already been reported.[29] Anti-inflammatory molecule in general prevents NF-κB translocation to nucleus. To further evaluate the effect of compound **4b** on huMIF-induced translocation of NF-κB to nucleus, electrophoretic mobility shift assay (EMSA) was performed. The isolated nuclear extracts (proteins) from the control, huMIF-induced and **4b** (2–80 μM) pretreated huMIF-induced RAW 264.7 cell were checked by EMSA. The translocation of NF-κB was not found as no complex was visible in labeled DNA (NF-κB consensus sequence) in absence of nuclear extract (Fig. 2 lane 1) and in presence of control nuclear extract (Fig. 2, lane 2). However, increased NF-κB translocation was observed after huMIF treatment as evident from the shifting of band due to complex formation (Fig. 2, lane 3).The data indicated that compound **4b** concentration-dependently inhibited huMIF-mediated translocation of NF-κB as evident from reduced complex formation (Fig. 2, lanes 4–7).

2.2.4. Compound 4b inhibits huMIF-mediated expression of pro-inflammatory nitric oxide synthase (iNOS) and NO production

NF-κB translocation to the nucleus is one of the important factor for up regulation of many pro-inflammatory cytokines and induction of inducible nitric oxide synthase (iNOS) gene.[29,30] Since **4b** prevents huMIF-mediated translocation of NF-κB to nucleus, we measured huMIF-mediated iNOS and its stable product nitrite (NO_2^-) production in RAW 264.7 cells in presence and absence of **4b**. The results indicate that **4b** (50 μM) significantly inhibits huMIF-induced up regulation of iNOS (Fig. 3A) and supported the EMSA finding. huMIF shows almost 61% increase in iNOS production in vitro in comparison to the control (without huMIF treatment) (Fig. 3A), whereas the compound **4b** treatment significantly decreases huMIF-induced iNOS production to almost half of the induced one (Fig. 3A). Since up-regulation of iNOS promotes nitric oxide (NO) production,[31] we further checked the effect of **4b** (50 μM) on huMIF-induced NO production in RAW 264.7 cells. The data clearly indicate that huMIF increases the NO production as expected and **4b** treatment decreases it significantly as shown in Figure 3B.

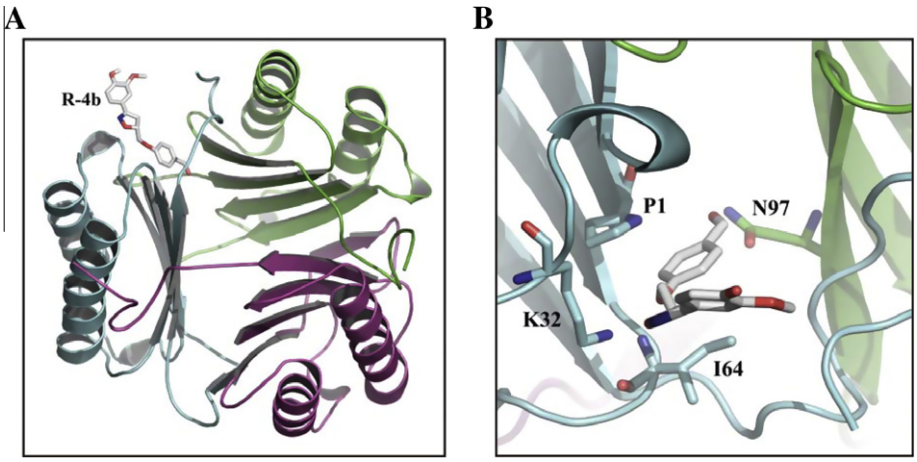

Figure 1. (A) Ribbon diagram of huMIF homotrimer docked with the compound *R*-**4b**. Each monomer is indicated by a different color. (B) Magnified view of the *R*-**4b** binding site. Docked conformation produced by AutoDock 4 indicates that the compound *R*-**4b** complexed with huMIF active sites through the side chains of Lys32, Ile64 and Asn97 from two neighboring subunits. Pro1 might be involved as indicated by the PatchDock. The figures were generated using PyMOL.

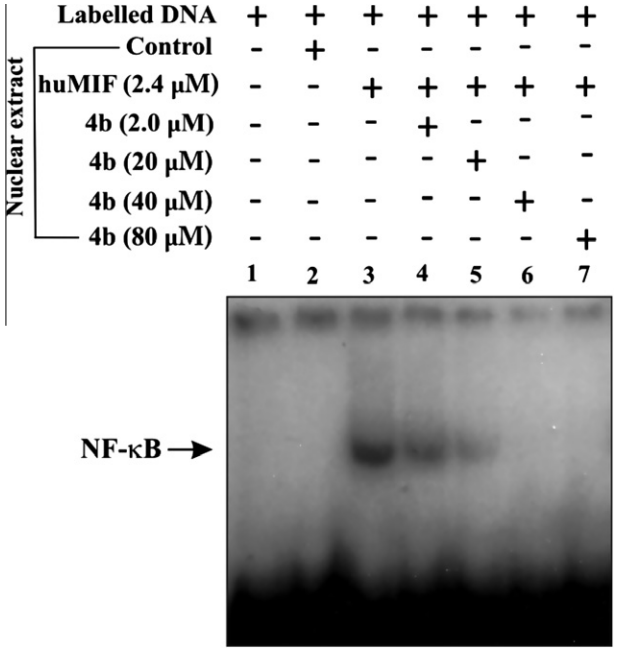

Figure 2. Protective effect of **4b** on huMIF-induced NF-κB translocation from cytosol to nucleus in vitro. Nuclear proteins isolated from RAW 264.7 cells of control and huMIF treated and **4b** pretreated huMIF induced were used for electrophoretic mobility shift assay (EMSA) as described under 'Section 4'. Lane 1, only labeled DNA; lane 2, control nuclear protein; lanes 3–7, nuclear proteins isolated from **4b** pretreated huMIF treated cells.

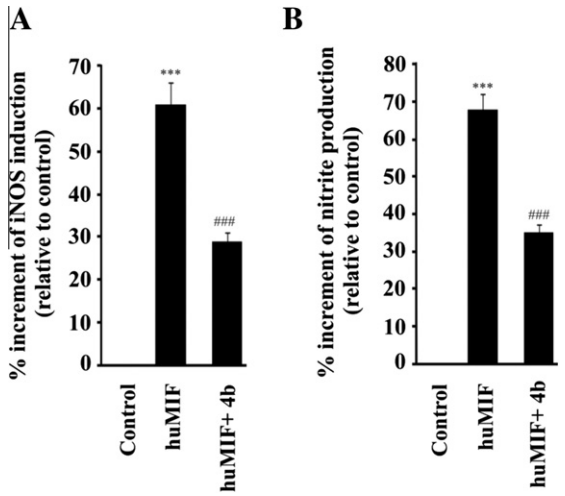

Figure 3. (A) Protective effect of **4b** on huMIF-mediated up regulation of iNOS. (B) Protective effect of **4b** on huMIF-mediated nitrite (NO_2^-) production. The details of the methodology were described under 'Section 4'. Data were presented as mean ± SEM ($***$ = P <0.001 vs control, $^{###}$ = P <0.001 vs. MIF, n = 6).

2.3. Cytotoxicity

From the above experiments it is clear that **4b** is effective against huMIF induced inflammation in vitro in cellular system. Now, the question arises whether this compound **4b** is toxic to the cells or not. To check the toxicity of **4b**, cell viability was monitored by following 3-(4,5-dimethylthiazol-2-yl)-2,5-diphenyltetrazolium bromide (MTT) assay as described earlier.[32] This assay was performed in RAW 264.7 cells as well as primary cultured gastric mucosal cells. In this assay, viability of the cells was determined by the reduction of the yellow MTT into purple formazan product by mitochondrial dehydrogenase present in metabolically active cells. Percent viability of the cells was calculated from the

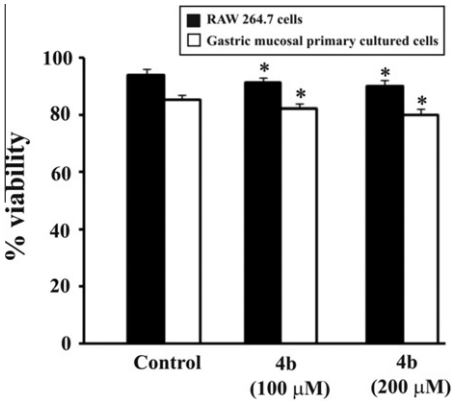

Figure 4. Evaluation of cytotoxicity. % viability of **4b** as measured in RAW 264.7 cells and gastric mucosal primary cultured cells by MTT assay. Data were presented as mean ± SEM ($*$ <0.05 vs control, n = 6).

absorbance of produced formazan dye. Data indicate that % viability of the cells are almost equivalent to the control cells in the **4b** treated RAW 264.7 cells as well as primary cultured gastric mucosal cells (Fig. 4) even at concentration which is more than 25-fold excess (200μM) to IC_{50} value (200 μM). From this experiment, it is evident that **4b** is not a cytotoxic molecule and could be exploited for further anti-inflammatory drug development.

The compound **4b** is more or less same potent as previously reported compound containing isoxazoline skeleton (e.g., ISO-1) to inhibit the tautomerase activity of huMIF in vitro. However, the dose for compound **4b** required to inhibit NF-κB translocation to the nucleus induced by the huMIF is lesser than the well known isoxazoline skeleton containing compound ISO-1. This may be due to higher Log$P$ value for **4b** (cLog$P$ 2.72) compared to ISO-1 (cLog$P$ 1.22). Log$P$ value is an estimate of a compounds overall lipophilicity that influences its behaviour in a range of biological processes such as solubility, membrane permeability, lack of selectivity and non-specific toxicity. cLog$P$ values were computed at Virtual Computational Chemistry Laboratory server (http://www.vcclab.org/lab/alogps/ as on October 14, 2011) with ALOGPS 2.1 program.[33] The reported dose for the inhibition of NF-κB translocation to the nucleus by ISO-1 is almost 70% at 100 μM,[23] whereas our data show that the compound **4b** inhibits almost 100% translocation between the range of 40–80 μM (Fig. 2). Therefore, compound **4b** could be a good candidate for the drug discovery against the huMIF induced pro-inflammatory diseases.

3. Conclusion

In summary, we have synthesized a new non-toxic molecule **4b**, that inhibits tautomerase activity of huMIF and attenuates huMIF-mediated translocation of NF-κB to nucleus. **4b** also prevents huMIF-mediated up regulation of iNOS and then NO production, which are well established factors for inflammation. Thus, from these experiments, we suggest that the compound **4b** might be beneficial for treatment of huMIF-induced inflammatory diseases.

4. Experimental section

4.1. Chemistry

4.1.1. General

All reactions using moisture or oxygen sensitive reagents were run under argon atmosphere with exclusion of moisture using standard techniques. Analytical thin-layer chromatography (TLC) was performed on TLC aluminum sheets 20 × 20 cm Silica Gel 60

F_{254} (Merck). The developed chromatogram was visualized under UV light (366, 254 nm). For purification, column chromatography was performed using 60–120 mesh silica gels (SRL).

^1H and ^{13}C NMR spectra were recorded using a Bruker Advance 300 or 600 MHz and signals were represented in parts per million from tetramethylsilane with the solvent resonance used as the internal standard [$CDCl_3$: ^1H NMR δ = 7.26 ppm (singlet); ^{13}C NMR δ = 77.0 ppm (triplet), DOSO-d_6]. Data were reported as follows: chemical shift, multiplicity (s = singlet, d = doublet, dd = doublet of doublet, t = triplet, m = multiplet and br s = broad singlet, ddd = doublet of double doublet), coupling constant (in Hz) and integration. All ^{13}C NMR spectra were obtained with complete proton decoupling. ^{13}C peak assignment is based on DEPT experiment. Mass spectra were obtained from ESI-TOF. IR spectra were recorded in KBr plate. Melting points were uncorrected.

4.2. General procedure for the preparation of various oxime

To a solution of $NH_2OH{\cdot}HCl$ (1.2 equiv, 36 mmol) dissolved in minimum volume of water, NaOAc was added (1.5 equiv, 45 mmol) portion wise at 0 °C, and the mixture was stirred for 30 min at room temperature. The appropriate aldehyde such as 4-hydroxy benzaldehyde, *p*-anisaldehyde, vanilin, 3,4-dimethoxy benzaldehyde (1 equiv 30 mmol each) dissolved in methanol (50 mL) was then added to the solution and stirring was continued for an additional 12 h until completion of reaction as indicated by TLC. Methanol was evaporated in vacuo and the residue extracted with ethylacetate, washed with water. The organic layer was washed with brine solution, dried and evaporated to dryness. Compounds were isolated as solid powder or semi solid.

4.3. General procedure for the preparation of various isoxazole derivatives

To a solution of oxime (1 equiv, 20 mmol) in anhydrous DMF (20 mL), NCS (1.5 equiv, 30 mmol) was added. The reaction mixture was stirred for 5 h at room temperature. To this solution, alkene (2 equiv, 40 mmol) in DMF (10 mL) was added, followed by dropwise addition of triethylamine (1.5 equiv, 30 mmol) in DMF (10 mL). The reaction mixture was stirred under N_2 at room temperature for 48 h until completion as indicated by TLC.

4.3.1. 2-(3-(4-Hydroxyphenyl)-4,5-dihydroisoxazol-5-yl)acetic acid (1a)

The crude product was purified by silica gel column chromatography using 70% ethyl acetate in hexane as eluents to give **1a** (48%). R_f: 0.53 (ethyl acetate); ^1H NMR (300 MHz, acetone-d_6) δ 2.65–2.76 (m, 2H), 3.13–3.24 (m, 1H), 3.51–3.62 (m, 1H), 5.0–5.09 (m, 1H), 6.9 (d, 1H, *J* = 8.4 Hz), 7.09 (d, 1H, *J* = 8.4 Hz), 7.52–7.59 (m, 2H), 7.98 (s, 1H); ^{13}C NMR (75 MHz, acetone-d_6) δ 39.41, 39.49, 77.47, 115.63, 116.69, 121.47, 128.32, 128.40, 156.20, 162.73, 171.25; MS (ESI) *m/z* calcd for $C_{11}H_{11}NO_4$: 221.07; found: 244.71 $[M+Na]^+$.

4.3.2. 2-(3-(4-Methoxyphenyl)-4,5-dihydroisoxazol-5-yl)acetic acid (1b)

The crude product was purified by silica gel column chromatography using 40% ethyl acetate in hexane as eluents to yield **1b** (64%). R_f: 0.517 (60% ethyl acetate in hexane); ^1H NMR (300 MHz, acetone-d_6) δ 2.66–2.82 (m, 2H), 3.15–3.26 (m, 1H), 3.52–3.63 (m, 1H), 3.96 (s, 3H), 5.01–5.10 (m, 1H), 6.99 (d, 1H, *J* = 8.7 Hz), 7.18 (d, 1H, *J* = 8.7 Hz), 7.64 (t, 2H, *J* = 7.2 Hz), 10.51 (br s, 1H); ^{13}C NMR (75 MHz, acetone-d_6) δ 39.17, 39.24, 55.87, 77.46, 112.48, 114.07. 126.77, 127.07, 127.99, 155.88, 161.87, 170.87; HRMS (ESI) *m/z* $(M+Na)^+$ calcd for $C_{12}H_{13}NO_4Na$: 258.0742; found: 258.0742.

4.3.3. 2-(3-(4-Hydroxy-3-methoxyphenyl)-4,5-dihydroisoxazol-5-yl)acetic acid (1c)

The crude product was purified by silica gel column chromatography using 70% ethyl acetate in hexane as eluents to provide **1c** (52%). R_f: 0.55 (ethyl acetate); ^1H NMR (300 MHz, acetone-d_6) δ 2.77–2.82 (m, 2H), 3.14–3.25 (m, 1H), 3.51–3.63 (m, 1H), 3.93 (s, 3H), 5.01–5.10 (m, 1H), 6.87 (d, 1H, *J* = 8.1 Hz), 7.11(d, 1H, *J* = 8.1 Hz), 7.22 (s, 1H), 10.59 (br s, 1H); ^{13}C NMR (75 MHz, acetone-d_6) δ 39.25, 39.51, 55.97, 77.87, 107.94, 109.51, 120.99, 144.92, 148.74, 155.86, 156.51, 171.30. MS(ESI) *m/z* calcd for $C_{12}H_{13}NO_5$: 251.08; found: 274.07 $[M+Na]^+$.

4.3.4. Methyl 3-(3,4-dimethoxyphenyl)-4,5-dihydroisoxazole-5-carboxylate (2a)

^1H NMR (300 MHz, $CDCl_3$) δ 3.6–3.63 (m, 2H), 3.80 (s, 3H), 3.90 (s, 6H), 5.12–5.18 (m, 1H), 6.85 (d, 1H, *J* = 8.34 Hz), 7.04 (dd, 1H, J_1 = 8.34 Hz, J_2 = 1.8 Hz), 7.37 (d, 1H, *J* = 1.92 Hz); ^{13}C NMR (75 MHz, $CDCl_3$) δ 36.85, 52.98, 56.20 (2C), 77.85, 109.33,110.88, 120.84, 121.54, 149.48, 151.48, 156.01, 171.05; MS (ESI) *m/z* calcd for $C_{13}H_{15}NO_5$: 265.09; found: 288.08 $[M+Na]^+$.

4.3.5. 1-(3-(3,4-Dimethoxyphenyl)-4,5-dihydroisoxazol-5-yl)ethanone (2b)

^1H NMR (300 MHz, $CDCl_3$) δ 2.10 (s, 3H), 3.41–3.64 (m, 2H), 3.90 (s, 6H), 4.96–5.02 (m, 1H), 6.85 (dd, 1H, J_1 = 8.51 Hz, J_2 = 1.8 Hz), 7.05 (dd, 1H, J_1 = 8.49 Hz, J_2 = 1.95 Hz), 7.34 (d, 1H, *J* = 1.83 Hz); ^{13}C NMR (75 MHz, $CDCl_3$) δ 26.50, 37.52, 56.38, 77.87, 84.45, 109.03, 110.80, 120.86, 121.47, 149.39, 151.41, 156.51, 207.95. MS (ESI) *m/z* calcd for $C_{13}H_{15}NO_4$: 249.1; found: 272.08 $[M+Na]^+$.

4.3.6. *N*-(2-(5-Methoxy-1*H*-indol-3-yl)ethyl)-2-(3-(4-methoxyphenyl)-4,5-dihydroisoxazol-5-yl)acetamide (3a)

^1H NMR (300 MHz, $CDCl_3$) δ 2.42–2.59 (m, 2H), 2.90–2.93 (m, 2H), 2.97–3.07 (m, 1H), 3.34–3.46 (m, 1H), 3.55 (t, 2H, *J* = 6.1 Hz), 3.81 (s, 3H), 3.82 (s, 3H), 4.94–4.99 (m, 1H), 6.28 (br s, 1H), 6.80–6.85 (m, 3H), 7.00 (d, 2H, *J* = 7.2 Hz), 7.21 (d, 1H, *J* = 8.7 Hz), 7.51 (d, 1H, *J* = 8.4 Hz), 7.98 (s, 1H), 8.34 (br s, 1H); ^{13}C NMR (75 MHz, $CDCl_3$) δ 25.08, 39.58, 39.83, 41.63, 55.28, 55.85, 77.79, 100.31, 111.80, 112.17, 114.08 (2C), 121.55, 122.80, 123.05, 126.37, 127.57, 128.39 (2C), 131.47, 153.85, 156.32, 174.51; MS (ESI) *m/z* calcd for $C_{23}H_{25}N_3O_4$: 407.18; found: 430.18 $[M+Na]^+$.

4.3.7. *N*-(4-Hydroxy-5-isopropyl-2-methylphenyl)-2-(3-(4-methoxyphenyl)-4,5-dihydroisoxazol-5-yl)acetamide (3b)

^1H NMR (300 MHz, $CDCl_3$) δ 1.14–1.18 (m, 6H), 2.12 (s, 3H), 2.75–2.84 (m, 2H), 3.05–3.12 (m, 1H), 3.18–3.26 (m, 1H), 3.50–3.59 (m, 1H), 3.84 (s, 3H), 5.12–5.15 (m, 1H), 6.50 (s, 1H), 6.92 (d, 2H, *J* = 7.8 Hz), 7.24 (d, 2H, *J* = 7.8 Hz), 7.59 (s, 1H); ^{13}C NMR (75 MHz, $CDCl_3$) δ 14.18, 22.50, 22.91, 26.88, 40.01, 40.34, 42.31, 55.38, 60.42, 77.85, 114.17 (2C), 114.22, 117.09, 121.51, 126.52, 130.19, 132.46, 150.77, 157.05, 161.32, 174.65; MS (ESI) *m/z* calcd for$C_{22}H_{26}N_2O_4$: 382.19; found: 405.14 $[M+Na]^+$.

4.3.8. 2-Isopropyl-5-methylphenyl 2-(3-(4-methoxyphenyl)-4,5-dihydroisoxazol-5-yl)acetate (3c)

^1H NMR (300 MHz, $CDCl_3$) δ 1.22 (d, 6H, *J* = 6.6 Hz), 2.31 (s, 3H), 2.87–3.01 (m, 2H), 3.09–3.24 (m, 2H), 3.55–3.64 (m, 1H) 3.95 (s, 3H), 5.19–5.24 (m, 1H), 6.82 (s, 1H), 6.96 (d, 2H, *J* = 8.4 Hz), 7.03 (d, 1H, *J* = 7.5 Hz), 7.20 (d, 1H, *J* = 7.8 Hz), 7.63 (d, 2H, *J* = 7.63 Hz); MS (ESI) *m/z* calcd for $C_{22}H_{25}NO_4$: 367.18; found: 390.12 $[M+Na]^+$.

4.3.9. 4-Acetamidophenyl 2-(3-(4-methoxyphenyl)-4,5-dihydroisoxazol-5-yl)acetate (3d)

^1H NMR (300 MHz, $CDCl_3$) δ 2.10 (s, 3H), 2.82 (dd, 1H, J_1 = 14.7 Hz, J_2 = 6.9 Hz), 3.11(dd, 1H, J_1= 16.65 Hz, J_2 = 6.6 Hz), 3.41–3.56 (m, 2H), 3.77 (s, 3H), 5.11 (br s, 1H), 6.51 (br s, 1H),

6.86 (t, 4H, J = 7.8 Hz), 7.53 (d, 1H, J = 8.7 Hz), 7.53(d, 1H, J = 8.7 Hz), 7.64 (s,1H); MS (ESI) m/z calcd for $C_{20}H_{20}N_2O_5$: 368.14; found: 391.17 $[M+Na]^+$.

4.3.10. Methyl 2-(3-(4-methoxyphenyl)-4,5-dihydroisoxazol-5-yl)acetate (3e)[20]

^{1}H NMR (300 MHz, $CDCl_3$) δ 2.64 (dd, 1H, J_1 = 16.5 Hz, J_2 = 6 Hz), 2.87 (dd, 1H, J_1 = 15.00 Hz, J_2 = 6.0 Hz), 3.09 (dd, 1H, J_1 = 16.5 Hz, J_2 = 9 Hz), 3.49–3.58 (m, 2H), 3.84 (s, 3H), 3.94 (s, 3H), 5.03–5.13 (m, 1H), 6.92 (d, 2H, J = 8.7 Hz), 7.60 (d, 1H, J = 8.7 Hz); MS (ESI) m/z calcd for $C_{13}H_{15}NO_4$: 249.1; found: 272.09 $[M+Na]^+$.

4.3.11. Butyl 2-(3-(4-methoxyphenyl)-4,5-dihydroisoxazol-5-yl)acetate (3f)[20]

^{1}H NMR (300 MHz, $CDCl_3$) δ 0.93 (t, 3H, J = 7.3 Hz),1.32–1.44 (m, 2H), 1.57–1.66 (m, 2H), 2.51–2.66 (m, 1H), 2.86 (dd, 1H, J_1 = 16.05 Hz, J_2 = 5.7 Hz), 3.09 (dd, 1H, J_1 = 16.5 Hz, J_2 = 7.2 Hz), 3.47–3.64 (m, 1H), 3.83 (s, 3H), 4.12 (t, 2H, J = 6.6 Hz), 5.02–5.12 (m, 1H), 6.91 (d, 2H, J = 8.7 Hz), 7.19 (d, 2H, J = 8.7 Hz); ^{13}C NMR (75 MHz, $CDCl_3$) δ 13.61, 19.04, 30.51, 39.80, 40.42, 55.29, 64.72, 77.38, 114.07 (2C), 121.90, 128.17 (2C), 156.01, 161.06, 170.29. MS (ESI) m/z calcd for $C_{16}H_{21}NO_4$: 291.15; found: 314.17 $[M+Na]^+$.

4.3.12. 4-(5-((2-Isopropyl-5-methylphenoxy)methyl)-4,5-dihydroisoxazol-3-yl)-2-methoxyphenol (4a)

^{1}H NMR (300 MHz, acetone-d_6) δ 1.06 (d, 3H, J = 6.9 Hz), 1.09 (d, 3H, J = 6.9 Hz), 2.26 (s, 3H), 3.13–3.22 (m, 1H), 3.38–3.45 (m, 1H), 3.54–3.64 (m, 1H), 3.89 (s, 3H), 4.12–4.18 (m, 2H); 5.04–5.11 (m,1H), 6.70 (d, 1H, J = 7.5 Hz), 6.77 (s, 1H), 6.88 (d, 1H, J = 8.4 Hz), 7.03 (d, 1H, J = 7.5 Hz), 7.14 (d, 1H, J = 8.1 Hz), 7.83 (s, 1H), 8.05 (s, 1H) MS (ESI) m/z calcd for $C_{21}H_{25}NO_4$: 355.43; found: 378.14 $[M+Na]^+$.

4.3.13. 4-((3-(4-Hydroxy-3-methoxyphenyl)-4,5-dihydroisoxazol-5-yl) methoxy) benzaldehyde (4b)

^{1}H NMR (300 MHz, acetone-d_6) δ 3.38–3.46 (m, 1H), 3.58–3.67 (m, 1H), 3.94 (s, 3H), 4.3 (d, 2H, J = 4.5 Hz), 5.11–5.13 (m, 1H), 7.14–7.19 (m, 4H), 7.39 (d, 1H, J = 1.2 Hz), 7.88 (d, 2H, J = 8.4 Hz), 9.90 (s, 1H); ^{13}C NMR (75 MHz, acetone-d_6) δ 36.88, 55.46, 69.31, 78.37, 107.87, 114.80 (3C), 120.61, 122.67, 130.40, 131.44 (2C),145.88, 147.62, 155.93, 163.52, 190.14; MS (ESI) m/z calcd for $C_{18}H_{17}NO_5$: 327.11; found: 350.09 $[M+Na]^+$.

4.3.14. Bis-isoxazoline derivative (5a)

^{1}H NMR (300 MHz, $CDCl_3$) δ 2.62–2.70 (m, 1H), 2.85–2.97 (m, 2H), 3.03–3.26 (m, 3H), 3.45–3.65 (m, 2H) 3.73 (s, 3H), 3.86 (s, 3H), 5.11–5.23 (m, 2H), 6.95 (d, 2H, J = 7.8 Hz), 7.21 (d, 2H, J = 7.8 Hz), 7.47–7.70 (m, 4H); MS (ESI) m/z calcd for $C_{24}H_{24}N_2O_7$: 452.16; found: 475.12 $[M+Na]^+$.

4.4. Biochemical evaluation methods

4.4.1. Cloning, over-expression and purification of huMIF

Cloning, over expression and purification of the huMIF protein was performed as described earlier by Bernhagen et al.[34] Briefly, the full length cDNA clone of huMIF was obtained from ORIGENE, USA which was cloned into pCMV6-XL5 cloning vector. MIF from complete ORF from the clone pCMV6-XL5 was PCR amplified with forward primer 5' CTTCTGCCATATGCCGATG 3' (*NdeI* restriction site was underlined) and reverse primer 5' CTCGAGATAGGCGAAGGTG 3' (*XhoI* restriction site was underlined). PCR cycling was as follows: 94 °C for 8 min, then 35 cycles of denaturation at 94 °C for 1 min, annealing at 49 °C for 1 min and extension at 72 °C for 1 min; and final extension at 73 °C for 8 min. PCR product was analyzed through electrophoresis on a 1% agarose gel in Tris-acetate-EDTA at 10 volts/cm. For cloning purpose *Escherichia coli* expression vector pET21b was used. PCR amplified huMIF gene was then purified by MiniElute® PCR purification kit (Qiagen) to remove the remaining of the PCR reaction mixture. Purified huMIF gene and pET21b vector were digested with fast digest restriction endonuclease *Nde1-XhoI* (Fermentas) for 30 min and subjected to ligation in an optimized molar ratio of 1:10 (vector: insert). Ligation was performed by rapid DNA ligation kit (Fermentas) for 15 min, followed by transformation in competent DH5α cells using the procedure as described earlier.[35,36] Transformants were screened through the colony PCR and positive clones were reconfirmed by PCR and restriction digestion as described earlier.[37] Cloning of complete ORF of huMIF was finally confirmed by sequencing of the clone. For the over-expression and purification of huMIF, essentially same procedure was adopted as described earlier for the *Pf*MIF.[35] For the measurement of final endotoxin concentration in purified huMIF protein, a chromogenic *Limulus* amoebocyte assay was used. Purified huMIF was found containing no more than trace amounts of LPS (7–10 ng of LPS/mg of huMIF).

4.4.2. Preparation of L-dopachrome methyl ester and tautomerase assay

Tautomerase activity of huMIF was determined at room temperature by adding a final concentration of 0.75 mM L-dopachrome methyl ester as described earlier.[38,39] Briefly, L-dopachrome methyl ester was prepared by mixing 4 mM L-3,4-dihydroxyphenylalanine methyl ester with 8 mM of sodium periodate for 5 min at room temperature and then placed directly on ice for 20 min before use. Activity was determined at 25 °C by adding dopachrome methyl ester to a cuvette containing 60 nM huMIF in 10 mM potassium phosphate buffer, pH 6.2 and 0.5 mM EDTA. The activity was monitored by measuring the conversion of L-dopachrome methyl ester to indolecarboxylic acid methyl ester at 475 nm for 20 s. To see the effect of synthesized compounds on tautomerase activity, the inhibitors were dissolved in DMSO at various concentrations and added to the cuvette with the huMIF prior to the addition of the dopachrome.

4.5. Molecular modeling

The crystal structure of huMIF (PDB ID: 1GD0) was obtained from Protein Data Bank (www.pdb.org). The two stereo-isomers of **4b** were drawn in GaussView 3.0 and energy minimized with HF/STO-3G* level of theory using GAUSSIAN 03. AutoDock 4.2[40] along with MGLTools[41] of The Scripps Research Institute was used as the principal tool for the docking calculations. The results were verified with PatchDock.[42] The later uses different algorithms from that of AutoDock, that include geometric patch detection on the molecular surface, surface patch matching, filtering and scoring. AutoDock 4, on the other hand, provides a choice of several methods for doing the conformation search: Genetic Algorithm (GA), Simulated Annealing, Local Search (LS) and Lamarckian GA-LS combination.[40]

On the local machine, docking calculations were carried out with AutoDock 4.2. Protein and the ligands were prepared with MGLTools. Gasteiger partial charges were added. Non-polar hydrogen atoms were merged, and rotatable bonds were defined. The whole receptor molecule was placed in a grid box with 0.775 Å grid point spacing and set to rigid. The preliminary blind docking experiment suggested binding site(s), where, in the final run smaller grid boxes were placed only to encompass those regions. Torsions were allowed to the long side chains of the amino acid residues in the vicinity of the ligand. Docking simulations were performed using the Lamarckian genetic algorithm (LGA) and the Solis & Wets local search method. Initial position, orientation, and torsions of the ligand molecules were set randomly. All rotatable torsions were released during docking. Each docking experiment was derived from 100 independent runs each of which was set to terminate after a

maximum of 25,000,000 energy evaluations. The population size was set to 150.

The PyMOL [http://www.pymol.org] molecular viewer and the MGLTools[41] were used to render the output and to calculate the distances between atoms. The Accessible Surface Area (ASA) of the ligands, protein and the complexes were computed by Mark Gerstein's calc-surface program on Helix Systems server of NIH (http://helixweb.nih.gov/structbio/) using 1.4 Å probe size. The least energy docked conformations were chosen. The changes in ASA of the ligands and the protein upon complex formation were calculated.

4.6. Macrophage cell culture

The mouse monocyte/macrophage cell line RAW 264.7 was maintained in RPMI 1640 (Sigma) supplemented with 100 U/mL penicillin, 100 μg/mL streptomycin, 10 μg/mL gentamycin, and 10% heat-inactivated fetal bovine serum. The cells were kept in a 37 °C incubator with 5% CO_2. Cells were sub cultured by scraping when plates reached 90% confluence with a 1:5 ratio in fresh medium. For iNOS and NO production assay, cells were seeded at a density of 2.5×10^6 cells mL^{-1}, whereas for NF-κB translocation assay 5×10^7 cells mL^{-1} was used in 6-well plates 12 h prior to treatment (viability of cell counts were carried out by trypan blue staining using a hemocytometer). The cells were then treated with 50 μM of test compound **4b** for 30 min prior to the addition of huMIF (100 nM). Cells were then again kept on incubation for an additional 24 h at 37 °C in CO_2 incubator for iNOS and NO production and 4 h for the NF-κB translocation assay. For every experiment, one positive control (cells treated only with huMIF) and one negative control (cells without any treatment) were included. Duplicate of each treated and control were taken for each experiment.

4.7. Gastric mucosal cell culture

Gastric mucosal cells were isolated and cultured as described earlier[32,43–45] with slight modification. Mucosa from rat stomach was scraped into HBSS (pH 7.4) containing 100 U/mL penicillin and 100-μg/mL streptomycin. The mucosa was then minced and suspended in HBSS (pH 7.4), containing 0.05% hyaluronidase and 0.1% collagenase type I. The suspension was incubated for 30 min at 37 °C in 5% CO_2 environment with shaking and then filtered through a sterile nylon mesh. The filtrate was centrifuged at 600*g* for 5 min, the cell pellet was washed with HBSS (pH 7.4) and further centrifuged. The pellet was incubated in 5 ml of Ham's F-12 media in T25 flask supplemented with 10% fetal bovine serum (FBS) and 100 U/mL penicillin, 100-μg/mL streptomycin and 10 μg/mL gentamycin. Cells were cultured at 37 °C with 5% CO_2 and grown to ~90% confluence before treatment. 90% of the cells, obtained following this protocol, possessed epithelial characteristics.[32]

4.8. Electrophoretic mobility shift assay (EMSA) to follow NF-kB translocation

To follow the effect of huMIF on NF-kB translocation, RAW cells were treated with or without MIF. RAW cells treated with **4b** (2–80 μM) 30 min prior to the huMIF (100 nM) treatment (post MIF treated) were used to check the effect of **4b** on huMIF activity. Cells were then collected after 4hrs of huMIF treatment and washed twice with PBS (pH 7.4). Nuclear extracts from control (RAW cells), huMIF treated and post huMIF treated RAW cells were isolated using ProteoJET™ Cytoplasmic and Nuclear Protein Extraction kit (Fermentas, USA) according to the manufacturer's instruction. The NF-κB consensus sequence (Promega) was annealed to create double-stranded and 5′-end-labeled with [γ-^{32}P] ATP using T4 polynucleotide kinase, according to standard protocols. Unincorporated [γ-^{32}P] ATP was removed by ethanol precipitation at −20 °C (overnight) followed by washing with 70% ethanol. Reactions were performed in a volume of 20 μL containing ^{32}P-labeled ds NF-κB consensus sequence (50 nM) incubated with nuclear extract from above mentioned groups (80 μg) in binding buffer (10 mM HEPES buffer, pH 7.6, 50 mM NaCl, 1 mm EDTA, 5 mM $MgCl_2$, 0.1 mM dithiothreitol, 1 mg/mL BSA and 0.05% Triton X-100) for 30 min on ice. NF-kB-oligo complexes were then separated by native gel electrophoresis (5%) running under 10 V/cm at 4 °C with 0.5X TBE (Tris/borate/EDTA; 1X TBE = 45 mM Tris/borate and 1 mM EDTA) running buffer. The gel was dried and exposed to an X-ray film overnight at −80 °C before film development.

4.9. Assay for the induction of inducible nitric oxide synthase (iNOS)

The RAW 264.7 cells were seeded overnight in a 24-well plate at a density of 2.5×10^6 cells mL^{-1}. The cells were pre-treated with either 50 μM of **4b** or were left untreated, for 30 min. These pre-treated and untreated cells were then stimulated with 100 nM MIF for 24 h, and the inhibition of iNOS induction in the cells was quantitatively assayed using Nitric Oxide Synthase Detection System, Fluorimetric (Sigma) kit according to the manufacturer's instructions. RAW cells without any treatment were used as control. The assay plate was analyzed in a HITACHI F-7000 fluorescence spectrophotometer at an excitation wavelength of 490 nm and an emission wavelength of 520 nm.

4.10. Assay for nitric oxide (NO) release

Direct measurement of nitric oxide (NO) production is difficult. For NO estimation, nitrite (NO_2^-) and nitrate (NO_3^-), the stable products of NO oxidation, were measured in biological fluids and cell culture medium. The supernatant of the control, huMIF-treated (100 nM) and **4b** (50 μM) pre-treated huMIF-treated RAW 264.7 cells were collected and stored quickly at −80 °C. The released NO_2^- in the medium was measured using Griess reagent (a 1:1 mixture of 0.1% naphthylethylenediamine dihydrochloride and 1% sulfanilamide in 5% H_3PO_4) as an indicator of NO formation.[46] Triplicate aliquots of cell-free culture supernatants were mixed with an equal volume of Griess reagent. After 10 min, the absorbance was taken at 570 nm in a microplate reader.

4.11. Cytotoxicity assay

Basic protocol for cytotoxicity assay was same as described earlier.[32] This assay for cell viability is based on the reduction of MTT by mitochondrial dehydrogenase in viable cells to produce a purple formazan product which shows the linearity between optical density and cell number. RAW 264.7 (1×10^6 cells/well in 24-well plates) and primary cultured gastric mucosal cells (1×10^6 cells/well in 24-well plates) were incubated with **4b** (100–200 μM) for 24 h. Then the medium was removed and 400 μl of fresh medium was added along with 100 μl of MTT (5 mg/mL). After 4 h of incubation with MTT, purple crystals were produced in the medium. These crystals were dissolved in DMSO (1 mL). The absorbance was measured at test wavelength of 550 nm and a reference wavelength of 620 nm. From the absorbance % viability of the cells was calculated. Data represent means ± SEM of two experiments done in duplicates.

4.12. Statistical analysis

All data are presented as means ± SEM. Data were analyzed as applicable by unpaired Student's *t* test with a two-tailed

distribution or by one-way ANOVA followed by multiple comparison *t* tests for evaluation of differences between groups. *p* value of $\leqslant 0.05$ was considered significant.

Acknowledgments

We thank Council of Scientific and Industrial Research (CSIR) New Delhi, University Grants Commission (UGC) New Delhi, University of Burdwan and Department of Science and Technology (DST) for providing fellowship to carry out the work. We also thank Dr. Santu Bandyopadhyay, Division of Infectious Diseases and Immunology, IICB, Kolkata for his kind gift of RAW 264.7 cells.

Supplementary data

Supplementary data associated with this article can be found, in the online version, at doi:10.1016/j.bmc.2011.10.056.

References and notes

1. Bernhagen, J.; Calandra, T.; Bucala, R. *Biotherapy* **1994**, *8*, 123.
2. Calandra, T.; Roger, T. *Nat. Rev. Immunol.* **2003**, *3*, 791.
3. Bloom, B. R.; Bennett, B. *Science* **1966**, *153*, 80.
4. David, J. R. *Proc. Natl. Acad. Sci. U.S.A.* **1966**, *56*, 72.
5. Rossi, A. G.; Haslett, C.; Hirani, N.; Greening, A. P.; Rahman, I.; Metz, C. N.; Bucala, R.; Donnelly, S. C. *J. Clin. Invest.* **1998**, *101*, 2869.
6. Imamura, K.; Nishihira, J.; Suzuki, M.; Yasuda, K.; Sasaki, S.; Kusunoki, Y.; Tochimaru, H.; Takekoshi, Y. *Biochem. Mol. Biol. Int.* **1996**, *40*, 1233.
7. Nishihira, J.; Koyama, Y.; Mizue, Y. *Cytokine* **1998**, *10*, 199.
8. Bacher, M.; Metz, C. N.; Calandra, T.; Mayer, K.; Chesney, J.; Lohoff, M.; Gemsa, D.; Donnelly, T.; Bucala, R. *Proc. Natl. Acad. Sci. U.S.A.* **1996**, *93*, 7849.
9. Calandra, T.; Bernhagen, J.; Mitchell, R. A.; Bucala, R. *J. Exp. Med.* **1994**, *179*, 1895.
10. Conroy, H.; Mawhinney, L.; Donnelly, S. C. *QJM* **2010**, *103*, 831.
11. Mitchell, R. A.; Metz, C. N.; Peng, T.; Bucala, R. *J. Biol. Chem.* **1999**, *274*, 18100.
12. Kithcart, A. P.; Cox, G. M.; Sielecki, T.; Short, A.; Pruitt, J.; Papenfuss, T.; Shawler, T.; Gienapp, I.; Satoskar, A. R.; Whitacre, C. C. *FASEB J.* **2010**, *24*, 4459.
13. Santos, L. L.; Morand, E. F. *Clin. Chim. Acta* **2009**, *399*, 1.
14. Ramanujam, M.; Davidson, A. *Expert Rev. Mol. Med.* **2008**, *10*, e2.
15. Ouertatani-Sakouhi, H.; El-Turk, F.; Fauvet, B.; Cho, M. K.; Pinar Karpinar, D.; Le Roy, D.; Dewor, M.; Roger, T.; Bernhagen, J.; Calandra, T.; Zweckstetter, M.; Lashuel, H. A. *J. Biol. Chem.* **2010**, *285*, 26581.
16. Vera, P. L.; Iczkowski, K. A.; Howard, D. J.; Jiang, L.; Meyer-Siegler, K. L. *Neurourol. Urodyn.* **2010**, *29*, 1451.
17. Lubetsky, J. B.; Dios, A.; Han, J.; Aljabari, B.; Ruzsicska, B.; Mitchell, R.; Lolis, E.; Al-Abed, Y. *J. Biol. Chem.* **2002**, *277*, 24976.
18. Cross, J. V.; Rady, J. M.; Foss, F. W.; Lyons, C. E.; Macdonald, T. L.; Templeton, D. J. *Biochem. J.* **2009**, *423*, 315.
19. Fingerle-Rowson, G.; Kaleswarapu, D. R.; Schlander, C.; Kabgani, N.; Brocks, T.; Reinart, N.; Busch, R.; Schutz, A.; Lue, H.; Du, X.; Liu, A.; Xiong, H.; Chen, Y.; Nemajerova, A.; Hallek, M.; Bernhagen, J.; Leng, L.; Bucala, R. *Mol. Cell. Biol.* **2009**, *29*, 1922.
20. Cheng, K. F.; Al-Abed, Y. *Bioorg. Med. Chem. Lett.* **2006**, *16*, 3376.
21. Dios, A.; Mitchell, R. A.; Aljabari, B.; Lubetsky, J.; O'Connor, K.; Liao, H.; Senter, P. D.; Manogue, K. R.; Lolis, E.; Metz, C.; Bucala, R.; Callaway, D. J.; Al-Abed, Y. *J. Med. Chem.* **2002**, *45*, 2410.
22. Xue, C. B.; Wityak, J.; Sielecki, T. M.; Pinto, D. J.; Batt, D. G.; Cain, G. A.; Sworin, M.; Rockwell, A. L.; Roderick, J. J.; Wang, S.; Orwat, M. J.; Frietze, W. E.; Bostrom, L. L.; Liu, J.; Higley, C. A.; Rankin, F. W.; Tobin, A. E.; Emmett, G.; Lalka, G. K.; Sze, J. Y.; Di Meo, S. V.; Mousa, S. A.; Thoolen, M. J.; Racanelli, A. L.; Olson, R. E., et al *J. Med. Chem.* **1997**, *40*, 2064.
23. Al-Abed, Y.; Dabideen, D.; Aljabari, B.; Valster, A.; Messmer, D.; Ochani, M.; Tanovic, M.; Ochani, K.; Bacher, M.; Nicoletti, F.; Metz, C.; Pavlov, V. A.; Miller, E. J.; Tracey, K. J. *J. Biol. Chem.* **2005**, *280*, 36541.
24. Wityak, J.; Sielecki, T. M.; Pinto, D. J.; Emmett, G.; Sze, J. Y.; Liu, J.; Tobin, A. E.; Wang, S.; Jiang, B.; Ma, P.; Mousa, S. A.; Wexler, R. R.; Olson, R. E. *J. Med. Chem.* **1997**, *40*, 50.
25. Balachandran, S.; Rodge, A.; Gadekar, P. K.; Yadav, V. N.; Kamath, D.; Chetrapal-Kunwar, A.; Bhatt, P.; Srinivasan, S.; Sharma, S.; Vishwakarma, R. A.; Dagia, N. M. *Bioorg. Med. Chem. Lett.* **2009**, *19*, 4773.
26. Balachandran, S.; Gadekar, P. K.; Parkale, S.; Yadav, V. N.; Kamath, D.; Ramaswamy, S.; Sharma, S.; Vishwakarma, R. A.; Dagia, N. M. *Bioorg. Med. Chem. Lett.* **2011**, *21*, 1508.
27. Swope, M.; Sun, H. W.; Blake, P. R.; Lolis, E. *EMBO J.* **1998**, *17*, 3534.
28. Holden, N. S.; Catley, M. C.; Cambridge, L. M.; Barnes, P. J.; Newton, R. *Eur. J. Biochem.* **2004**, *271*, 785.
29. Amin, M. A.; Haas, C. S.; Zhu, K.; Mansfield, P. J.; Kim, M. J.; Lackowski, N. P.; Koch, A. E. *Blood* **2006**, *107*, 2252.
30. Guzik, T. J.; Korbut, R.; Adamek-Guzik, T. J. *Physiol. Pharmacol.* **2003**, *54*, 469.
31. Oh, J. H.; Lee, T. J.; Park, J. W.; Kwon, T. K. *Eur. J. Pharmacol.* **2008**, *599*, 11.
32. Pal, C.; Bindu, S.; Dey, S.; Alam, A.; Goyal, M.; Iqbal, M. S.; Maity, P.; Adhikari, S. S.; Bandyopadhyay, U. *Free Radical Biol. Med.* **2010**, *49*, 258.
33. Tetko, I. V.; Bruneau, P. *J. Pharm. Sci.* **2004**, *93*, 3103.
34. Bernhagen, J.; Mitchell, R. A.; Calandra, T.; Voelter, W.; Cerami, A.; Bucala, R. *Biochemistry* **1994**, *33*, 14144.
35. Alam, A.; Goyal, M.; Iqbal, M. S.; Bindu, S.; Dey, S.; Pal, C.; Maity, P.; Mascarenhas, N. M.; Ghoshal, N.; Bandyopadhyay, U. *Free Radical Biol. Med.* **2011**, *50*, 1659.
36. Choubey, V.; Guha, M.; Maity, P.; Kumar, S.; Raghunandan, R.; Maulik, P. R.; Mitra, K.; Halder, U. C.; Bandyopadhyay, U. *Biochim. Biophys. Acta* **2006**, *1760*, 1027.
37. Guha, M.; Choubey, V.; Maity, P.; Kumar, S.; Shrivastava, K.; Puri, S. K.; Bandyopadhyay, U. *Protein Expr. Purif.* **2007**, *52*, 363.
38. Kamir, D.; Zierow, S.; Leng, L.; Cho, Y.; Diaz, Y.; Griffith, J.; McDonald, C.; Merk, M.; Mitchell, R. A.; Trent, J.; Chen, Y.; Kwong, Y. K.; Xiong, H.; Vermeire, J.; Cappello, M.; McMahon-Pratt, D.; Walker, J.; Bernhagen, J.; Lolis, E.; Bucala, R. *J. Immunol.* **2008**, *180*, 8250.
39. Aroca, P.; Solano, F.; Garcia-Borron, J. C.; Lozano, J. A. *Biochem. J.* **1991**, *277*, 393.
40. Morris, G. M.; Huey, R.; Lindstrom, W.; Sanner, M. F.; Belew, R. K.; Goodsell, D. S.; Olson, A. J. *J. Comput. Chem.* **2009**, *30*, 2785.
41. Sanner, M. F. *J. Mol. Graph. Model.* **1999**, *17*, 57.
42. Schneidman-Duhovny, D.; Inbar, Y.; Nussinov, R.; Wolfson, H. J. *Nucleic Acids Res.* **2005**, *33*, W363.
43. Maity, P.; Bindu, S.; Dey, S.; Goyal, M.; Alam, A.; Pal, C.; Mitra, K.; Bandyopadhyay, U. *J. Biol. Chem.* **2009**, *284*, 3058.
44. Maity, P.; Bindu, S.; Choubey, V.; Alam, A.; Mitra, K.; Goyal, M.; Dey, S.; Guha, M.; Pal, C.; Bandyopadhyay, U. *J. Biol. Chem.* **2008**, *283*, 14391.
45. Maity, P.; Bindu, S.; Dey, S.; Goyal, M.; Alam, A.; Pal, C.; Reiter, R.; Bandyopadhyay, U. *J. Pineal Res.* **2009**, *46*, 314.
46. Gharavi, N.; El-Kadi, A. O. *J. Pharm. Pharm. Sci.* **2003**, *6*, 302.